

Blue-Phase Liquid Crystal Displays With Vertical Field Switching

Hui-Chuan Cheng, Jin Yan, Takahiro Ishinabe, Norio Sugiura, Chu-Yu Liu, Tai-Hsiang Huang, Cheng-Yeh Tsai, Ching-Huan Lin, and Shin-Tson Wu, *Fellow, IEEE*

Abstract—A low-voltage, high-transmittance, hysteresis-free, and submillisecond-response polymer-stabilized blue-phase liquid crystal (BPLC) display with vertical field switching (VFS) and oblique incident light is demonstrated. In the VFS mode, the electric field is in longitudinal direction and is uniform. By using a thin cell gap and a large oblique incident angle, the operation voltage is significantly reduced which plays a key role to eliminate hysteresis and residual birefringence. The VFS mode is a strong contender for the emerging BPLC display and photonic devices.

Index Terms—Blue phase liquid crystal (BPLC), hysteresis free, low voltage.

I. INTRODUCTION

POLYMER-STABILIZED blue-phase liquid crystal (PS-BPLC) [1]–[3] has potential to become next-generation display because it exhibits some attractive features, e.g., fast gray-to-gray response time [4], no need for alignment layer, and isotropic dark state. So far, almost all the BPLC devices utilize in-plane switching (IPS) electrodes [5], [6] in which the electric field is mainly in *lateral* direction and the Kerr effect-induced birefringence is along the electric field if the employed BPLC has a positive dielectric anisotropy ($\Delta\epsilon > 0$) [7]. Therefore, the backlight can be easily set at normal incidence and high contrast and wide view can be achieved fairly easily. However, IPS mode exhibits two shortcomings: high operating voltage and relatively large hysteresis. High operating voltage originates from that the electric fields are confined near the electrodes and do not penetrate deeply into the BPLC bulk [8]. Moreover, in an IPS mode the electric fields are nonuniform spatially. Near electrode edges, the electric fields are particularly strong which could cause lattice deformation, known as electrostriction effect, leading to hysteresis [9], [10]. To reduce voltage and hysteresis, some modified IPS structures such as protrusion electrodes [8], wall-shaped electrodes [11], double-penetrating fringe fields [12], and corrugated electrodes [13] have been proposed. Although these methods are helpful for reducing voltage, the device manufacturing process becomes more complicated.

Vertical field switching (VFS) has been recently proposed independently by Cheng *et al.* [14] and Kim *et al.* [15]. In [15], the

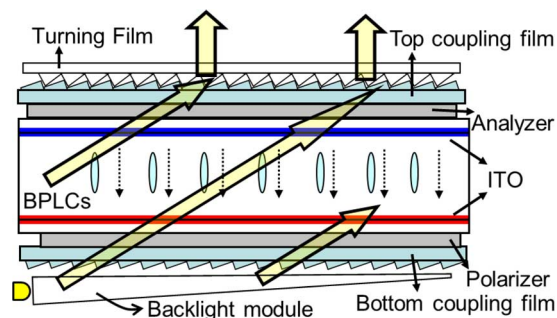


Fig. 1. Device structure of the proposed VFS-BPLCD.

normally incident backlight is split into oblique rays by a prism array before they impinge the BPLC cell. The device structure is fairly simple, but two problems remain to be overcome: double images and poor dark state because of the depolarization by the prisms between the polarizer and analyzer. While in [14], the incident light is set at $\sim 70^\circ$ so that the operating voltage is greatly reduced and hysteresis is completely suppressed. However, how to achieve wide view remains a challenge.

In this paper, we present the VFS mode BPLC in detail. Different from the IPS mode, the electric field in the VFS cell is in *longitudinal* direction and is uniform. By using a thin cell gap and a large oblique incident angle (70°), the operation voltage is reduced to ~ 10 V while eliminating the hysteresis. The uniform electric field also helps to reduce response time.

II. DEVICE STRUCTURE

Fig. 1 depicts the proposed VFS BPLC device structure. Because the electric field is in the longitudinal direction, only the incident light at an oblique angle ($0 < \theta < 90^\circ$) can experience the phase retardation effect. For a given BPLC layer thickness, a larger incident angle results in a larger phase retardation, which helps to lower the operating voltage. Therefore, we need to couple the backlight to a large output angle (e.g., $\theta \sim 70^\circ$) and keep it reasonably well collimated. The reason for having a well-collimated light is to achieve better viewing symmetry. If the incident light is not well collimated, then the portion with a smaller angle would accumulate less phase retardation and form lower gray levels, while the larger angle part would accumulate more phase retardation and form higher gray levels. After the light exits to the viewer's side, the divergent backlight would cause asymmetric brightness distribution when viewed from left-hand side or right-hand side of the panel. As a result, it will be difficult to obtain uniform brightness. This kind of collimated backlight which has large output angle is already adopted in some high brightness LCDs [16], [17]. The polarizer and analyzer are set at 45° and -45°

Manuscript received June 09, 2011; revised July 12, 2011; accepted August 02, 2011. Date of current version January 25, 2012.

H.-C. Cheng, J. Yan, T. Ishinabe, and S.-T. Wu are with the College of Optics and Photonics, University of Central Florida, Orlando, FL 32816 USA (e-mail: hccheng@creol.ucf.edu; swu@mail.ucf.edu).

N. Sugiura, C.-Y. Liu, T.-H. Huang, C.-Y. Tsai, and C.-H. Lin are with AU Optronics, Hsinchu 30078, Taiwan (e-mail: Teddy.TH.Huang@auo.com).

Color versions of one or more of the figures are available online at <http://ieeexplore.ieee.org>.

Digital Object Identifier 10.1109/JDT.2011.2164236

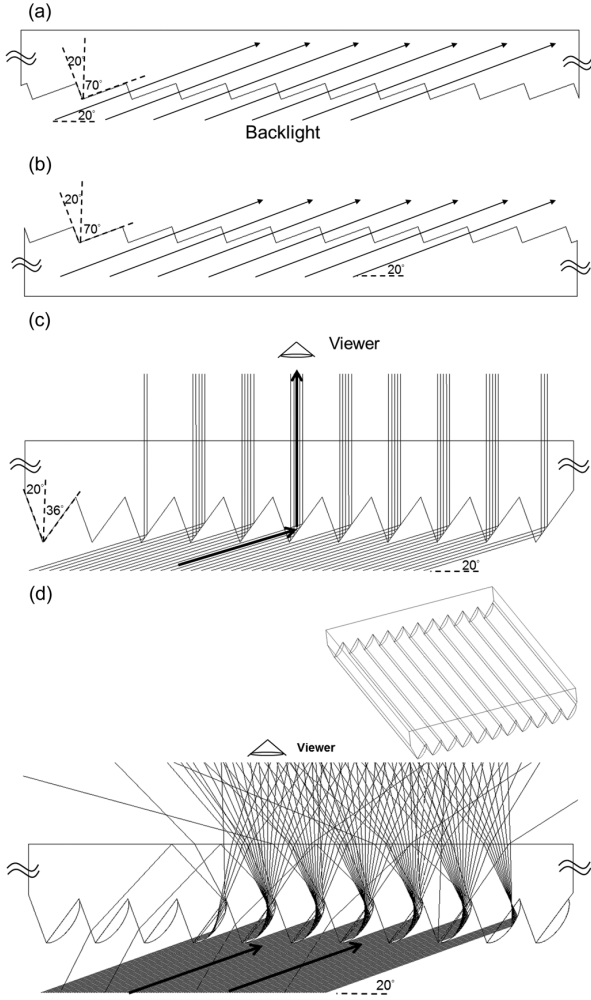


Fig. 2. Structures of (a) bottom coupling film; (b) top coupling film; (c) turning film with regular-angle prisms; and (d) turning film with round-shape prisms.

azimuthal angles. The prism films are set at 90° as shown in Fig. 1. We used the ray tracing software (i.e., LightTools) in our simulation. The refractive index of prism films is 1.59 and the thickness is $\sim 150 \mu\text{m}$. The backlight in our simulation has a Gaussian distribution for different polar angles. The maximum intensity is at 70° and FWHM is 30° .

Fig. 2(a) shows a bottom coupling film laminated on the bottom polarizer that can substantially couple the oblique incident light to the bottom substrate and the BPLC layer. It has a prismatic structure which not only couples the oblique input light to the cell but also keeps a large angle. If we do not use the bottom coupling film, the refraction angle in the BPLC layer will be reduced dramatically by Snell's law. As a result, the phase retardation will be smaller and the operating voltage will be higher. Therefore, the key for the VFS mode is to optimize the prism structure. From our simulation results, the prism structures with internal angles of 70° - 20° - 90° can substantially couple the $\sim 70^\circ$ incident light to the substrate without changing the light direction. The prism pitch should be smaller than each pixel size. Typically, it could range from $\sim 5 \mu\text{m}$ to $\sim 100 \mu\text{m}$.

Fig. 2(b) shows the structure of the top coupling film that is laminated on the top substrate. Its purpose is to couple the light

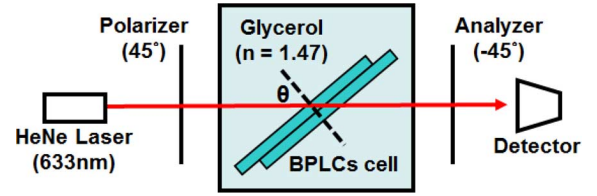


Fig. 3. Experimental setup for measuring the VFS cell.

to the air. Without top coupling film, the oblique angle light will be trapped in the cell module because of total internal reflection (TIR). The prism structures with internal angles of 70° - 20° - 90° can efficiently couple the light out of the substrate. A pair of coupling films plays an important role on keeping a large incident angle in the VFS LCDs. Fig. 2(c) shows the structure of the turning film. It steers the direction of the oblique light to the viewer's position by TIR without energy loss. The pitch of the turning film is designed to be the same as that of the top coupling film. Therefore, the turning film can be easily placed or laminated on the top coupling film. Because the light is still well collimated, the turning film with regular prisms is suitable for the narrow-view application. The angle of the turning film can be optimized according to the angle and profiles of the backlight. To realize wide viewing angle, we can use irregular prism, such as different prism angles to steer the backlight to multiple directions, or using the round shape prisms as shown in Fig. 2(d) to spread the light. The round shape prisms provide a wider viewing angle and more uniform image. It should also be more durable than triangular prisms.

III. EXPERIMENTS AND SIMULATIONS

We performed some experiments to confirm the advantages of our VFS device over the conventional IPS structure. Fig. 3 shows the experimental setup. To simulate the beam path shown in Fig. 1, we prepared a transparent container filled with Glycerol ($n = 1.47$ at $\lambda = 633 \text{ nm}$). The BPLC cell was immersed in Glycerol and it could be rotated freely. Because of matched index between glass and Glycerol, the light can pass through the BPLC in a very large angle.

We prepared a polymer-stabilized BPLC material using Chisso JC-BP01M [18]. The LC host has a birefringence $\Delta n \sim 0.17$ and dielectric anisotropy $\Delta\epsilon \sim 94$. The phase transition temperature of the precursor is BP 42.4°C N^* during the cooling process and N^* 44.5°C BP during the heating process, where N^* denotes chiral nematic phase. The phase transition temperature between blue phase and isotropic phase was not easy to determine precisely because Bragg reflection occurred at $\sim 350 \text{ nm}$. UV stabilization curing process was performed at 44°C for 30 min. with an intensity of 2 mW/cm^2 . After UV curing, the blue-phase temperature range was widened from $< 0^\circ\text{C}$ to $\sim 70^\circ\text{C}$. To make a fair comparison, we used the same material for both IPS and VFS cells. The IPS cell has patterned ITO electrodes with $10\text{-}\mu\text{m}$ electrode width and $10 \mu\text{m}$ electrode gap, and $7.5 \mu\text{m}$ cell gap. For the VFS cell, both top and bottom glass substrates were over-coated with a thin ITO electrode; no polyimide layer was used. The cell gap was $d \sim 5.74 \mu\text{m}$.

Fig. 4 depicts the measured voltage-dependent transmittance (VT) curves (at $\lambda = 633 \text{ nm}$ and $T \sim 23^\circ\text{C}$) of the IPS cell and

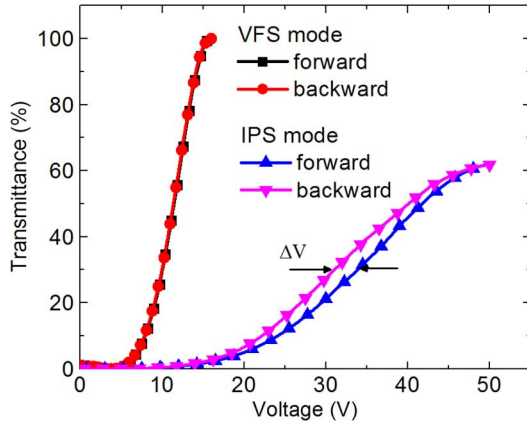


Fig. 4. Measured VT curves and hysteresis of IPS and VFS cells. $\lambda = 633$ nm.

VFS cell at $\theta = 70^\circ$. For the IPS cell measured at normal incidence, the peak voltage occurs at $V_p \sim 50 V_{rms}$. For the VFS cell at $\theta = 70^\circ$, its $V_p \sim 16 V_{rms}$ which is $\sim 3.2\times$ lower than that of IPS structure. To further reduce operating voltage, we could use a larger Kerr constant BPLC or increase the incident angle.

Hysteresis is a common phenomenon for polymer-stabilized liquid crystal devices [9]. For display applications, hysteresis affects the accuracy of gray scale control and should be eliminated. Hysteresis is defined by the voltage difference (ΔV) at half-maximum transmittance when we scan the voltage forward and backward. From Fig. 4, the measured $\Delta V/V_p$ is $\sim 5.8\%$ for the IPS cell. For our new VFS cell with $d = 5.74 \mu\text{m}$ and $\theta = 70^\circ$, it is free from hysteresis! The reason is because our VFS cell has a weak electric field ($E \sim 2.8 \text{ V}/\mu\text{m}$) so that the electrostriction effect does not occur. On the contrary, in an IPS cell the generated electric fields are not uniform spatially. The electric fields are much stronger near the pixel edges than those in the electrode gap. The peak electric fields could cause lattice deformation locally which results in hysteresis.

To validate this hypothesis, we applied different voltages (up to 40 V) to our VFS cell and measured their hysteresis at $\theta = 70^\circ$. Fig. 5 shows the field intensity versus corresponding phase retardation under the specified voltages. The black line represents the ascending curve, while red cycles, blue triangles, and green squares denote the descending curves from 40, 28, and 20 V, respectively. From Fig. 5, we find the accumulated phase increases almost linearly and then gradually saturates as the electric field exceeds $\sim 6 \text{ V}/\mu\text{m}$. For the $V = 20 V_{rms}$ curve ($E \sim 3.5 \text{ V}/\mu\text{m}$ in our $5.74\text{-}\mu\text{m}$ VFS cell), the forward and backward curves overlap very well and no hysteresis is observed. Therefore, the critical field (E_c) for a hysteresis-free BPLC using Chisso JC-BP01M is $\sim 3.5 \text{ V}/\mu\text{m}$. In our VFS cell, the electric field is uniform, thus it provides a reliable way for determining the critical field for a PS BPLC. On the other hand, for an IPS cell the electric field near electrode edges is often higher than $3.5 \text{ V}/\mu\text{m}$ so that it exhibits a noticeable hysteresis.

Residual birefringence is another serious problem for IPS BP-LCDs [19]. It causes light leakage at dark state and degrades the contrast ratio. In an IPS cell, the residual birefringence arises in the region with strong field. In a VFS cell, the required field intensity for producing 1π phase retardation is relatively weak. Thus, the resultant residual birefringence is negligible.

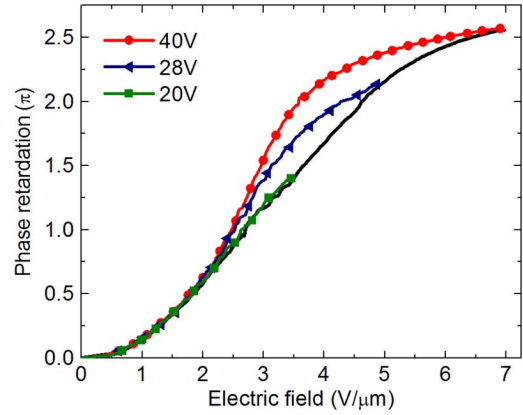


Fig. 5. Measured phase retardation vs. electric field intensity under different applied voltages. $\lambda = 633$ nm.

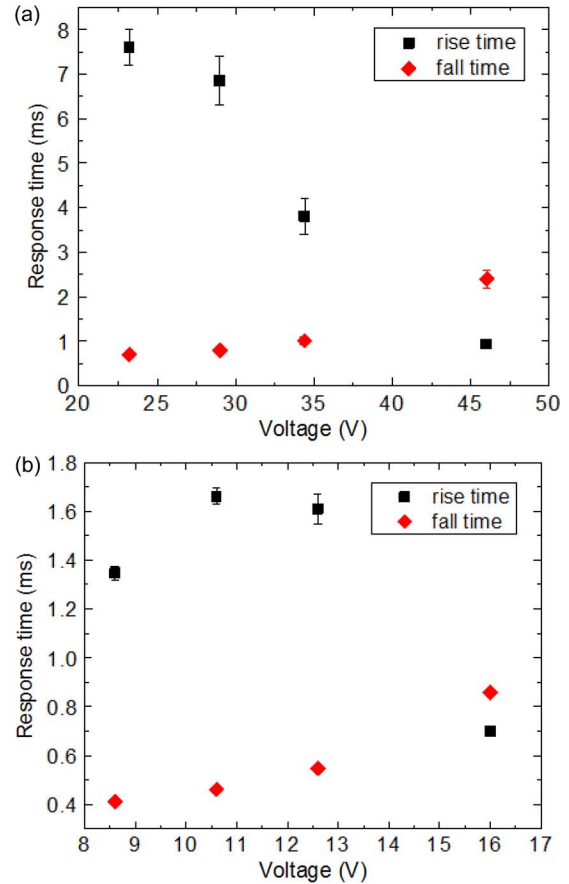


Fig. 6. Measured response time of (a) IPS cell and (b) VFS cell. $\lambda = 633$ nm.

We also compared the response time of our VFS cell with IPS cell at 23°C . Fig. 6(a) shows the gray-to-gray response time of the IPS cell while Fig. 6(b) shows the measured response time of our new VFS cell. The applied voltage swings from 0 to 16 V (@ 100 Hz) for the VFS cell, and 0 to ~ 46 V for the IPS cell. We find that our VFS mode shows much faster rise time and fall time as compared to the IPS cell. Again, this is attributed to the smaller LC reorientation angle and uniform field of the VFS cell.

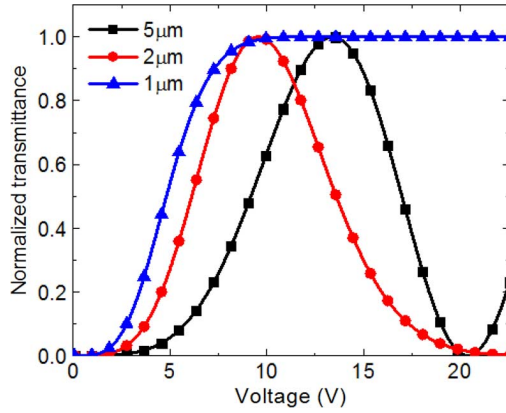


Fig. 7. Simulated VT curves under different cell gap ($d = 1 \mu\text{m}$, $2 \mu\text{m}$, and $5 \mu\text{m}$) for the VFS cell. Incident angle $= 70^\circ$ and $\lambda = 550 \text{ nm}$.

Unlike an IPS cell whose VT curve is insensitive to the cell gap, the peak transmittance voltage of our VFS cell is dependent on the cell gap. Here, two factors have to be considered: induced birefringence and effective cell gap. At a given voltage V , as the cell gap d decreases the electric field E gets stronger because $E = V/d$. According to Kerr effect, the induced birefringence is proportional to E^2 . Thus, the induced birefringence is larger as the cell gap decreases. On the other hand, for a given incident angle the beam path in the BPLC cell for accumulating phase retardation decreases as the cell gap decreases. Therefore, there ought to be an optimal cell gap for achieving certain phase retardation. If the cell gap is too thin, although the induced birefringence is large, the optical beam path is decreased so that the accumulated phase may not be adequate for achieving maximum transmittance. Moreover, the saturation phenomenon in the high field region should be also considered. In a real situation, the induced birefringence will gradually saturate as the electric field increases. Therefore, the driving voltage could not decrease indefinitely when we use an ultra-thin cell gap, as described by the extended Kerr effect equation [20].

In the extended Kerr effect model, the induced birefringence is expressed as follows:

$$\Delta n = \Delta n_{\text{sat}} \left(1 - \exp \left[- \left(\frac{E}{E_s} \right)^2 \right] \right) \quad (1)$$

where Δn_{sat} stands for the saturated induced birefringence and E_s represents the saturation field. From the measured results in Fig. 4, our polymer-stabilized BPLC material has $K \sim 7.5 \text{ nm/V}^2$ at $\lambda = 633 \text{ nm}$ in the low field region, with $\Delta n_{\text{sat}} \sim 0.17$ and $E_s \sim 6.0 \text{ V}/\mu\text{m}$. The Kerr constant extracted from VFS cell is $\sim 70\%$ smaller than that from IPS cell. A possible explanation is as follows. In an IPS cell, the electric field varies largely from electrode edges to the center of electrode gap. Therefore, the extracted Kerr constant thru curve fitting has a larger uncertainty.

Fig. 7 shows the simulated VT curves for $d = 5 \mu\text{m}$, $2 \mu\text{m}$, and $1 \mu\text{m}$ at $\lambda = 550 \text{ nm}$. For display applications, we often optimize the device design at $\lambda = 550 \text{ nm}$. To obtain the Kerr constant at this wavelength, we use the value measured at $\lambda = 633 \text{ nm}$ and then extrapolate it following the dispersion

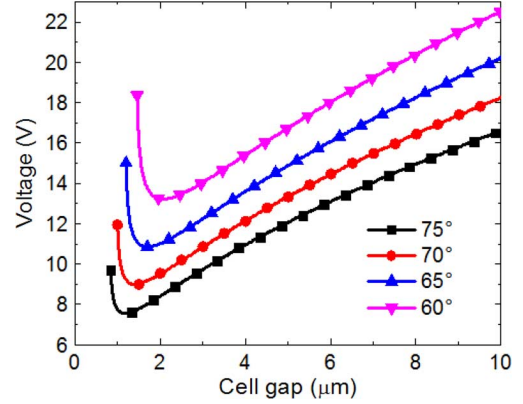


Fig. 8. Simulated operating voltage vs. cell gap at different incident angles of VFS cells. $\lambda = 550 \text{ nm}$ and Kerr constant is assumed to be $K \sim 7.5 \text{ nm/V}^2$.

relation [21]. For the $1\text{-}\mu\text{m}$ BPLC cell, the induced birefringence gradually saturates so that the maximum phase retardation reaches $\sim 1\pi$ at a fairly high voltage. As compared to the IPS structure whose VT curve is insensitive to the cell gap, the electro-optic effects of VFS are dependent on the cell gap. We can optimize the cell gap according to the material properties and incident angle to obtain a proper operation voltage. If we would compromise for a lower transmittance, we could use a thinner cell gap to trade for a lower operating voltage. For example, from Fig. 7 the $1\text{-}\mu\text{m}$ VFS cell has an operating voltage of 6 V at 70% transmittance, which is the typical transmittance of an IPS cell. If we want to boost the transmittance to 90% for the $1\text{-}\mu\text{m}$ VFS cell, then we can increase the operating voltage to 7.7 V . A caution should be taken that if we use a thinner cell gap to reduce driving voltage, the electric field might exceed the critical field (E_c) for causing hysteresis. The critical voltage for the $5 \mu\text{m}$, $2 \mu\text{m}$, and $1 \mu\text{m}$ cells is 17.5 , 7.0 , and 3.5 V , respectively.

Based on the extended Kerr effect, we simulated the cell gap versus the driving voltage at $\lambda = 550 \text{ nm}$ as shown in Fig. 8. As the cell gap decreases, the driving voltage decreases and then reaches a minimum. For the case of $\theta = 70^\circ$ and $d \sim 1.5 \mu\text{m}$, the minimum peak voltage occurs at $V_p \sim 9 \text{ V}$. As stated above, we can optimize cell gap according to the material properties and incident angle to obtain the minimum voltage. For the BPLC layer under a longitudinal field, the induced birefringence Δn is along the electric field and behaves as a C-plate [22]. The phase retardation Γ equals 1π for the first maximum transmittance and can be expressed as

$$\Gamma = \frac{2\pi}{\lambda} n_o d \left[\sqrt{1 - \frac{(n_g \sin \theta_0)^2}{n_e^2}} - \sqrt{1 - \frac{(n_g \sin \theta_0)^2}{n_o^2}} \right] = \pi \quad (2)$$

where d is the cell gap, n_g is the refractive index of Glycerol (Fig. 3), θ_0 is the incident angle, and n_o and n_e are the ordinary and extraordinary refractive indices of the BPLC. We also assume the following equations hold for n_o and n_e [20]:

$$n_o = n_i - \frac{1}{3} \Delta n; \quad n_e = n_i + \frac{2}{3} \Delta n \quad (3)$$

where n_i is the isotropic refractive index of BPLC in the voltage-off state, and Δn is the induced birefringence under an external electric field. After combining (1), (2), and (3), we

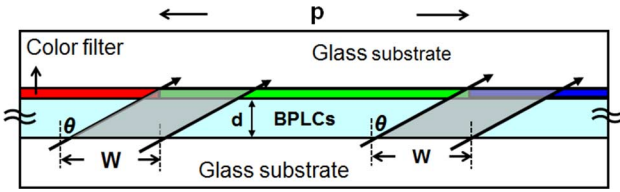


Fig. 9. Possible crosstalk in a VFS BP-LCD.

derive (by neglecting algebraic derivation) following analytical solution of cell gap d for the minimum operating voltage:

$$d = \frac{\lambda n_i \sqrt{n_i^2 - n_g^2 \sin^2 \theta}}{n_g^2 \sin^2 \theta \cdot \Delta n_s (\sqrt{5} - 1)} \quad (4)$$

The optical efficiency (normalized to two parallel polarizers) of an IPS BPLC cell is generally limited to $\sim 70\%$ due to some dead zones above the electrodes. Our VFS cell could in principle achieve 100% transmittance because of its uniform vertical fields without dead zones. The major optical loss comes from Fresnel reflection of the coupling films and turning films. From our simulations, the optical efficiency for the employed films is over 85%. Crosstalk between two adjacent pixels would also affect the transmittance of our VFS BPLC. As shown in Fig. 9, the width W of crosstalk equals $d/\cot \theta$, here d is the cell gap, and θ is the incident angle. Therefore, the transmittance ratio becomes $1 - W/p$, here p is each pixel width. Let us assume $d = 3 \mu\text{m}$, $\theta = 70^\circ$, and $p = 180 \mu\text{m}$, the transmittance would be 95%. We can fabricate TFT structure in the crosstalk region and add black matrix on it. Therefore, VFS should have a comparable or higher optical efficiency than IPS.

Achieving wide viewing angle is a major challenge for the VFS mode because the backlight's incident angle is fairly large. Since the backlight we used has a fairly narrow FWHM, this design is suitable for narrow-view applications. To widen the viewing angle, we can design irregular prism structure of turning film to orient backlight to multiple directions [14]. To spread the light more uniformly, a front diffuser could be considered [23]. We can also design more prism angles or use round-shape prisms to spread the light by TIR to get uniform brightness and high contrast ratio as shown in Fig. 2(d). The shape and angle of the micro prisms should be optimized according to the backlight profile employed.

IV. CONCLUSION

The VFS mode offers superior performances to IPS in lower operating voltage, higher transmittance, free from hysteresis, no residual birefringence, and faster response time. Its cell structure is very simple, but it requires sophisticated phase compensation scheme to achieve wide view. On the other hand, IPS requires protrusion electrodes to reduce operation voltage, but its phase compensation scheme for achieving wide view is relatively simple. The VFS mode is particularly attractive for display and photonic devices that require fast response time, such as field sequential color displays using RGB LED backlight.

ACKNOWLEDGMENT

The UCF group is indebted to Dr. Y. Haseba of Chisso for providing the BPLC material.

REFERENCES

- [1] H. Kikuchi, M. Yokota, Y. Hisakado, H. Yang, and T. Kajiyama, "Polymer-stabilized liquid crystal blue phases," *Nat. Mater.*, vol. 1, pp. 64–68, 2002.
- [2] Y. Haseba, H. Kikuchi, T. Nagamura, and T. Kajiyama, "Large electro-optic Kerr effect in nanostructured chiral liquid-crystal composites over a wide temperature range," *Adv. Mater.*, vol. 17, p. 2311, 2005.
- [3] J. Yan, L. Rao, M. Jiao, Y. Li, H. C. Cheng, and S. T. Wu, "Polymer-stabilized optically isotropic liquid crystals for next-generation display and photonic applications," *J. Mater. Chem.*, vol. 21, pp. 7870–7877, 2011.
- [4] K. M. Chen, S. Gauza, H. Xianyu, and S. T. Wu, "Submillisecond gray-level response time of a polymer-stabilized liquid crystal," *J. Display Technol.*, vol. 6, no. 2, pp. 49–51, Feb. 2010.
- [5] Z. Ge, S. Gauza, M. Jiao, H. Xianyu, and S. T. Wu, "Electro-optics of polymer-stabilized blue phase liquid crystal displays," *Appl. Phys. Lett.*, vol. 94, p. 101104, 2009.
- [6] Z. Ge, L. Rao, S. Gauza, and S. T. Wu, "Modeling of blue phase liquid crystal displays," *J. Display Technol.*, vol. 5, no. 7, pp. 250–256, Jul. 2009.
- [7] L. Rao, Z. Ge, and S. T. Wu, "Viewing angle controllable displays with a blue-phase liquid crystal cell," *Opt. Express*, vol. 18, pp. 3143–3148, 2010.
- [8] L. Rao, Z. Ge, S. T. Wu, and S. H. Lee, "Low voltage blue-phase liquid crystal displays," *Appl. Phys. Lett.*, vol. 95, p. 231101, 2009.
- [9] M. Sato and A. Yoshizawa, "Electro-Optical Switching in a blue phase III exhibited by a chiral liquid crystal oligomer," *Adv. Mater.*, vol. 19, p. 4145, 2007.
- [10] K. M. Chen, S. Gauza, H. Xianyu, and S. T. Wu, "Hysteresis effects in blue-phase liquid crystals," *J. Display Technol.*, vol. 6, no. 8, pp. 318–322, Aug. 2010.
- [11] M. Kim, M. S. Kim, B. G. Kang, M. K. Kim, S. Yoon, S. H. Lee, Z. Ge, L. Rao, S. Gauza, and S. T. Wu, "Wall-shaped electrodes for reducing the operation voltage of polymer-stabilized blue phase liquid crystal displays," *J. Phys. D: Appl. Phys.*, vol. 42, p. 235502, 2009.
- [12] L. Rao, H. C. Cheng, and S. T. Wu, "Low voltage blue-phase LCDs with double-penetrating fringe fields," *J. Display Technol.*, vol. 6, no. 8, pp. 287–289, Aug. 2010.
- [13] M. Jiao, Y. Li, and S. T. Wu, "Low voltage and high transmittance blue-phase liquid crystal displays with corrugated electrodes," *Appl. Phys. Lett.*, vol. 96, p. 011102, 2010.
- [14] H. C. Cheng, J. Yan, T. Ishinabe, and S. T. Wu, "Vertical field switching for blue-phase liquid crystal devices," *Appl. Phys. Lett.*, vol. 98, p. 261102, 2011.
- [15] Y. H. Kim, S. T. Hur, K. W. Park, D. H. Park, S. W. Choi, and H. R. Kim, "A vertical-field-driven polymer-stabilized blue phase liquid crystal displays," in *SID Symp. Dig.*, 2011, vol. 42, pp. 298–301.
- [16] M. Oe and I. Chiba, "Plane Light Source Unit," US Patent 5126882, 1992.
- [17] K. Kälälär, "A monolithic segmented functional light guide for 2-D dimming LCD backlight," *J. Soc. Inf. Display*, vol. 19, pp. 37–47, 2011.
- [18] L. Rao, J. Yan, S. T. Wu, S. Yamamoto, and Y. Haseba, "A large Kerr constant polymer-stabilized blue phase liquid crystal," *Appl. Phys. Lett.*, vol. 98, p. 081109, 2011.
- [19] H. Lee, H. J. Park, O. J. Kwon, S. J. Yun, J. H. Park, S. Hong, and S. T. Shin, "The world's first blue phase liquid crystal display," in *SID Symp. Dig.*, 2011, vol. 42, pp. 122–125.
- [20] J. Yan, H. C. Cheng, S. Gauza, Y. Li, M. Jiao, L. Rao, and S. T. Wu, "Extended Kerr effect in polymer-stabilized blue-phase liquid crystals," *Appl. Phys. Lett.*, vol. 96, p. 071105, 2010.
- [21] M. Jiao, J. Yan, and S. T. Wu, "Dispersion relation on the Kerr constant of a polymer-stabilized optically isotropic liquid crystal," *Phys. Rev. E.*, vol. 83, p. 041706, Apr. 2011.
- [22] X. Zhu, Z. Ge, and S. T. Wu, "Analytical solutions for uniaxial-film-compensated wide-view liquid crystal displays," *J. Display Technol.*, vol. 2, no. 1, pp. 2–20, Mar. 2006.
- [23] H. Takemoto, T. Fuchida, S. Shutou, and M. Miyatake, "The performance of collimated backlight and front diffusing systems on several LC modes," in *Proc. IDW'09*, 2009, pp. 1907–1908.

Hui-Chuan Cheng received the B.S. degree in electrical engineering and the M.S. degree in photonics in 2000 and 2005, respectively, from National Taiwan University, Taipei, Taiwan, and is currently working toward the Ph.D. degree from the College of Optics and Photonics, University of Central Florida (UCF), Orlando.

From 2005 to 2007, he was a senior engineer at AU Optronics, Hsinchu, Taiwan. His research interests include blue phase LCDs, sunlight readable LCDs, and touch panels.

Mr. Cheng is a recipient of 2011 SID distinguished student paper award. Currently, he is the president of SID student chapter at UCF.

Jin Yan is currently working toward the Ph.D. degree from the College of Optics and Photonics, University of Central Florida, Orlando.

Her research interest includes device physics and materials of polymer-stabilized blue phase and isotropic phase liquid crystal displays. She has 11 journal publications. Currently, she is the vice president of SID student chapter at UCF.

Takahiro Ishinabe received the B.S., M.S., and Ph.D. degrees in electronic engineering from Tohoku University, Sendai, Japan, in 1995, 1997, and 2000, respectively.

From 2000 to 2002, he was a Research Fellow of the Japan Society for the Promotion of Science, and since 2003, he has been an Assistant Professor in the Department of Electronics, Graduate School of Engineering, Tohoku University. Presently, he is a Visiting Professor at College of Optics and Photonics, University of Central Florida, researching on advanced liquid crystal displays.

Dr. Ishinabe is a recipient of the 2011 SID special recognition award. He is a member of Society for Information Display.

Norio Sugiura received the B.S., M.S., and Ph.D. degrees in electronic engineering from Tohoku University, Sendai, Japan, in 1993, 1995, and 1998, respectively.

Since 2005 he has been working at AU Optronics Corporation, Taiwan, where he is currently a director of Advanced Display Technology Research Center.

Dr. Sugiura is a member of Society for Information Display and International Liquid Crystal Society.

Chu-Yu Liu received the M.S. degree in materials science from National Tsing Hua University, Taiwan.

He has over 8 years of experiences in LCDs. He is a senior manager in Advanced Research Center of AU Optronics Corporation, Hsinchu, Taiwan. His recent research interests include blue phase LCD and flexible display.

Tai-Hsiang Huang received the M.S. degree in chemistry from National Tsing Hua University, Taiwan, and the Ph.D. degree in material science and engineering from National Chiao Tung University, in 2000 and 2006, respectively.

He has been a manager at AU Optronics since 2009. He has published more than 20 SCI papers and filed 8 patents. His research interests are in developing OLED and blue phase LC materials.

Cheng-Yeh Tsai received the M.S. degree in electrical-optical engineering from National Taiwan University, Taiwan, in 2003.

He was an advanced engineer at AU Optronics, Hsinchu, Taiwan. He has received 11 US patents and 9 Taiwan patents. His current research interests include blue-phase and field sequential LCDs.

Ching-Huan Lin received the B.S. and M.S. degrees in physics from National Cheng Kung University, Taiwan, in 1999 and 2001, respectively.

He has been a manager at AU Optronics since 2005. He received 37 US patents and 5 Japan patents. His current research interests include blue phase LCDs, transparent LCDs, and 3D displays.

Mr. Lin is a recipient of 2008 SID distinguished paper award.



Shin-Tson Wu (M'98–SM'99–F'04) received the B.S. degree in physics from National Taiwan University, and the Ph.D. degree from the University of Southern California, Los Angeles.

He is a Pegasus professor at College of Optics and Photonics, University of Central Florida.

Dr. Wu is the recipient of 2011 SID Slottow-Owaki prize, 2010 OSA Joseph Fraunhofer award, 2008 SPIE G. G. Stokes award, and 2008 SID Jan Rajchman prize. He was the founding Editor-in-Chief of IEEE/OSA JOURNAL OF DISPLAY TECHNOLOGY.

He is a Fellow of the Society of Information Display (SID), Optical Society of America (OSA), and SPIE.